The Tungsten–Tungsten Triple Bond. 14. Factors Influencing Triple Bonds between Tungsten Atoms Having Valence Molecular Orbital Configurations of $\sigma^2\pi^4$ and $\pi^4\delta^2$ and Preparation and Characterization of Bis(neopentyl)bis(acetato)-bis(diethyldithiocarbamato)ditungsten

Malcolm H. Chisholm,* David L. Clark, John C. Huffman, and William G. Van Der Sluys

Contribution from the Department of Chemistry and the Molecular Structure Center, Indiana University, Bloomington, Indiana 47405. *Received November 24, 1986*

Abstract: Compounds having the general formula $W_2R_2(O_2CX)_4$ (R = an alkyl lacking β hydrogens; X = alkyl, aryl, NR_2) adopt one of two basic structures with W–W triple bonds of approximate valence MO configurations of either $\pi^4\delta^2$ (I) or $\sigma^2\pi^4$ (II). The most common structure for X = alkyl or aryl is one in which the alkyl ligands, R, are aligned along the W–W axis and four O_2CX ligands span a W≡W bond of $\pi^4\delta^2$ configuration (I). The other structure, found exclusively for X = NR_2, is one in which there are mutually syn-alkyl ligands, and each W atom forms five W–L σ bonds that all lie roughly in a pentagonal plane with a resultant W≡W bond of $\sigma^2\pi^4$ configuration (II). Both steric and electronic factors are important in determining the choice of structure I or II. Bulky supporting ligands favor I and appear to show a discriminating factor R > X, but electronic factors can override these steric influences, as in the case of X = NR_2. The reaction between $W_2(np)_2(O_2CMe)_4$ (np = neopentyl) and NaS_2CNEt_2 (2 equiv) in hexane in the presence of MeCOOH yields $W_2(np)_2(O_2CMe)_2(S_2CNEt_2)_2$ with the transformation of the W≡W bond from $\pi^4\delta^2$ to $\sigma^2\pi^4$. The reaction between $W_2(np)_2(O_2CMe)_4$ and thioacetic *O*-acid (MeCOSH) yields $W_2(np)_2(O_2CMe)_3(SOCMe)$ with retention of the axial W–np ligands and the $\pi^4\delta^2$ configuration of the W≡W bond. With the aid of Fenske–Hall calculations we show that there is essentially no electronic energy barrier to the interconversion of $\pi^4\delta^2$ and $\sigma^2\pi^4$ triple bonds. Conjugation between carboxylate and N π lone-pair orbitals of carbamate ligands has a destabilizing influence on the δ orbital in the $\pi^4\delta^2$ manifold, rendering it unstable with respect to the $\sigma^2\pi^4$ configuration. A similar effect is invoked in the conversion of $W_2(np)_2(O_2CMe)_4$ to $W_2(np)_2(O_2CMe)_2(S_2CNEt_2)_2$. Pertinent distances (Å) for $W_2(np)_2(O_2CMe)_2(S_2CNEt_2)_2$ are W–W = 2.2909 (10) Å, W–O = 2.15 (1) Å (averaged), W–S = 2.52 (1) Å (averaged), and W–C = 2.19 (1) Å. Crystal data (−160 °C) are as follows: a = 17.092 (12) Å, b = 11.023 (7) Å, c = 17.576 (12) Å, β = 98.19 (4)°, d_{calcd} = 1.825 g cm^{-3}, Z = 4, and space group $P2_1/a$.

In the previous paper we describe the synthesis and characterization of a series of compounds of formula $M_2R_2(O_2CR')_4$ (M = Mo, W) having various combinations of R = methyl (Me), aryl (Ar), benzyl (Bz), and neopentyl (np) and R′ = H, Me, Et, *t*-Bu, and Ar.[1] The predominant structure of these compounds is depicted by I, though for R = Me, Bz, and Ar and R′ = H, Me,

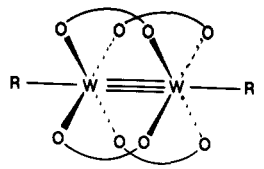

I

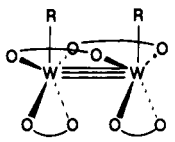

II

and Et an alternate structure II was also found to exist in solution. For R = Bz and Ar and R′ = Me and Et equilibrium mixtures of I and II exist in benzene-d_6 while for R and R′ = Me, II was the only isomer detected in solution by NMR spectroscopy.

The compounds that adopt structures of type I are closely related to the d^4–d^4 $W_2(O_2CR')_4$[2-5] compounds and we have shown that the valence MO description M–M $\pi^4\delta^2$ is common to both $W_2R_2(O_2CR')_4$ (type I) and $W_2(O_2CR')_4$.[1] By contrast the d^3–d^3 compounds of type II have W–W triple bonds of valence MO configuration $\sigma^2\pi^4$.[7-9] Note that in II, each tungsten atom forms five metal–ligand bonds that lie roughly in a pentagonal plane and will require that tungsten s, p_x, p_y, $d_{x^2-y^2}$, and d_{xy} atomic orbitals be used in metal–ligand σ bonding (defining the W–W axis as the z axis). It is therefore not possible to form a δ bond for II, whereas in I, the $d_{x^2-y^2}$ (or d_{xy}) tungsten orbital is available to form a δ bond.

What factors favor the adoption of the isomeric forms I and II? Obviously steric factors would seem to favor I relative to II when R, and to a lesser extent R′, are extremely bulky.[1] The compound $W_2(np)_2(O_2CH)_4$ was shown to adopt the structure type I both in the solid state and in solution.[1] However, electronic factors are also at work and as we show here the replacement of two carboxylate groups by two dithiocarbamate ligands can cause the preference of mutually syn-neopentyl ligands and the adoption of structure type II. We will compare this compound to other complexes of the formula $W_2R_2(O_2CNR_2')_4$ (R = Me, R′ = Et; R = Bz, np, R′ = Me) that also adopt structure type II,[7-9] and we offer an explanation for the electronic factors that favor II relative to I when X = NR'_2.

Results and Discussion

Synthesis of $W_2(np)_2(O_2CMe)_2(S_2CNEt_2)_2$. Hydrocarbon solutions of $W_2(np)_2(O_2CMe)_4$ react with NaS_2CNEt_2 in the presence of acetic acid according to eq 1.

$$W_2(np)_2(O_2CMe)_4 + 2NaS_2CNEt_2 \xrightarrow[\text{toluene/MeCO}_2\text{H}]{25\ ^\circ\text{C}} W_2(np)_2(O_2CMe)_2(S_2CNEt_2)_2 + 2NaO_2CMe \quad (1)$$

(1) Chisholm, M. H.; Clark, D. L.; Huffman, J. C.; Van Der Sluys, W. G.; Kober, E. M.; Lichtenberger, D. L.; Bursten, B. E. *J. Am. Chem. Soc.*, preceding article in this issue.
(2) Sattelberger, A. P.; McLaughlin, K. W.; Huffman, J. C. *J. Am. Chem. Soc.* **1981**, *103*, 2880.
(3) Santure, D. J.; McLaughlin, K. W.; Huffman, J. C.; Sattelberger, A. P. *Inorg. Chem.* **1983**, *22*, 1877.
(4) Santure, D. J.; Huffman, J. C.; Sattelberger, A. P. *Inorg. Chem.* **1985**, *24*, 371.
(5) Chisholm, M. H.; Chiu, H. T.; Huffman, J. C. *Polyhedron* **1984**, *6*, 759.
(6) Cotton, F. A.; Wang, W. *Inorg. Chem.* **1984**, *23*, 1604.
(7) Chisholm, M. H.; Cotton, F. A.; Extine, M. W.; Stults, B. R. *Inorg. Chem.* **1977**, *16*, 603.
(8) Chisholm, M. H.; Heppert, J. A. Hoffman, D. M.; Huffman, J. C. *Inorg. Chem.* **1985**, *24*, 3214.
(9) Chetcuti, M. J.; Chisholm, M. H.; Folting, K.; Haitko, D. A.; Huffman, J. C. *J. Am. Chem. Soc.* **1982**, *104*, 2138.

0002-7863/87/1509-6817$01.50/0

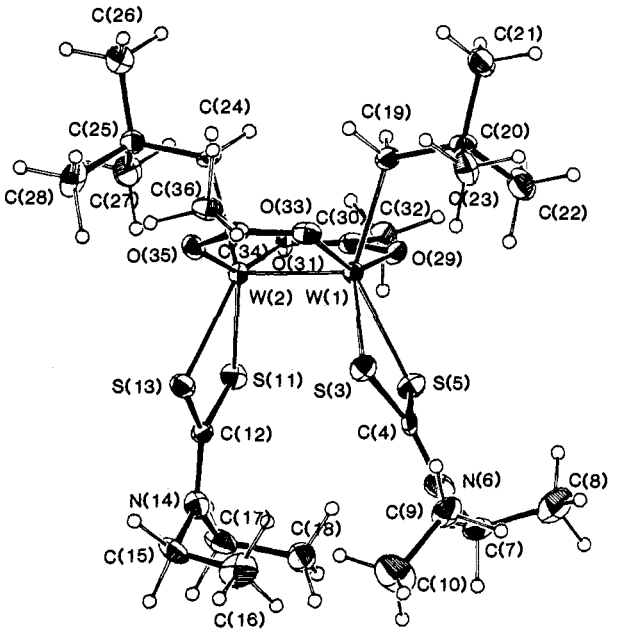

Figure 1. ORTEP view of the $W_2(np)_2(O_2CMe)_2(S_2CNEt_2)_2$ molecule giving the numbering scheme for the atoms used in the tables.

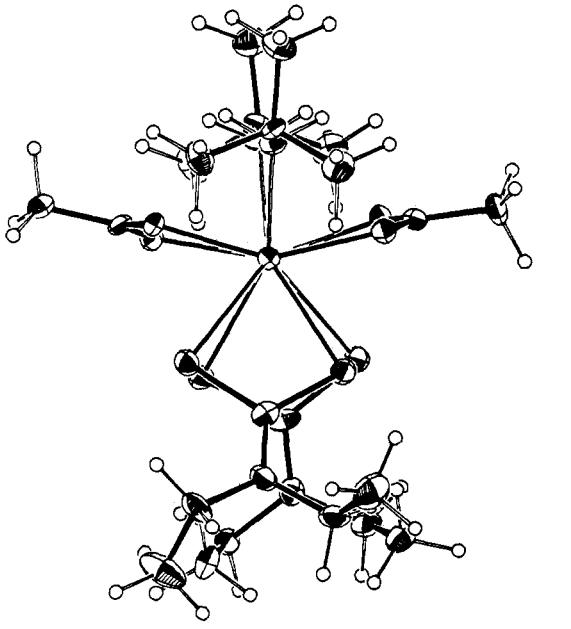

Figure 2. ORTEP view of the $W_2(np)_2(O_2CMe)_2(S_2CNEt_2)_2$ molecule looking along the W–W bond, emphasizing the near-eclipsed geometry of the two WL_5 pentagonal units.

$W_2(np)_2(O_2CMe)_2(S_2CNEt_2)_2$ is a yellow-orange, hydrocarbon-soluble, diamagnetic, air-stable, crystalline solid. It can be isolated in ca. 80% yield according to reaction 1 by crystallization from hexane.

Solid-State and Molecular Structure of $W_2(np)_2(O_2CMe)_2(S_2CNEt_2)_2$. An ORTEP view of $W_2(np)_2(O_2CMe)_2(S_2CNEt_2)_2$ giving the atom numbering scheme used in the tables is shown in Figure 1 and a view looking down the W–W bond is given in Figure 2. Atomic positional parameters are listed in Table I, and selected bond distances and angles are given in Tables II and III, respectively.

The molecule has virtual C_{2v} symmetry and the syn-neopentyl ligands are accommodated at the dinuclear center with seemingly little steric difficulty. The bulky *tert*-butyl groups are directed distal to the W–W bond and encounter no steric pressure from either the acetate or dithiocarbamate groups. The W–C, W–S, and W–O bonds lie roughly in a pentagonal plane, with the distortions being readily understood in terms of repulsions across the W–W bond and the bite of the bidentate and bridging ligands. The preference for bidentate S_2CNEt_2 and bridging O_2CMe no doubt reflects the larger bite of the S_2CNEt_2 ligand.

At this point is is worth noting that $W_2Me_2(O_2CNEt_2)_4$ was previously shown to adopt structure type II in the solid state.[7] The compound $W_2(np)_2(O_2CNMe_2)_4$, herein prepared, also adopts structure type II as evidenced by the two different carbamate

Table I. Fractional Coordinates and Isotropic Thermal Parameters for the $W_2(np)_2(O_2CMe)_2(S_2CNEt_2)_2$ Molecule

atom	10^4x	10^4y	10^4z	$10B_{iso}$, Å^2
W(1)	8691.3 (2)	2009.3 (3)	2016.9 (2)	13
W(2)	8326.8 (2)	1791.7 (3)	3214.3 (2)	13
S(3)	8704 (1)	−119 (2)	1500 (1)	19
C(4)	9704 (6)	−80 (8)	1575 (5)	16
S(5)	10090 (1)	1235 (2)	2021 (1)	19
N(6)	10148 (5)	−932 (7)	1319 (5)	21
C(7)	11003 (6)	−793 (10)	1288 (6)	26
C(8)	11512 (7)	−1522 (13)	1898 (8)	43
C(9)	9757 (6)	−2024 (9)	946 (6)	24
C(10)	9495 (8)	−1830 (11)	105 (7)	38
S(11)	9451 (1)	556 (2)	3911 (1)	19
C(12)	8889 (6)	−720 (8)	3737 (5)	17
S(13)	7938 (1)	−394 (2)	3336 (1)	18
N(14)	9161 (5)	−1840 (7)	3867 (5)	19
C(15)	8652 (6)	−2892 (9)	3631 (6)	24
C(16)	8625 (6)	−3235 (9)	2802 (6)	25
C(17)	10002 (6)	−2053 (9)	4161 (6)	23
C(18)	10523 (7)	−2075 (10)	3514 (7)	31
C(19)	8164 (6)	3710 (8)	1548 (5)	17
C(20)	8328 (6)	4050 (8)	745 (6)	18
C(21)	7900 (6)	5221 (10)	474 (6)	25
C(22)	9234 (6)	4249 (10)	751 (6)	24
C(23)	8048 (7)	3062 (10)	159 (6)	27
C(24)	7724 (6)	3499 (8)	3413 (8)	16
C(25)	7405 (6)	3606 (9)	4194 (5)	19
C(26)	6798 (7)	2639 (9)	4256 (6)	26
C(27)	8094 (6)	3460 (11)	4858 (6)	27
C(28)	7022 (7)	4836 (9)	4254 (6)	27
O(29)	9534 (4)	3371 (5)	2493 (4)	17
C(30)	9660 (6)	3523 (8)	3224 (5)	16
O(31)	9271 (4)	2981 (5)	3681 (4)	17
C(32)	10281 (6)	4419 (8)	3527 (6)	20
O(33)	7516 (4)	1497 (5)	1529 (4)	16
C(34)	6999 (6)	1321 (8)	1973 (6)	18
O(35)	7132 (4)	1483 (6)	2683 (3)	16
C(36)	6212 (6)	840 (9)	1627 (6)	22

Table II. Selected Bond Distances (Å) for the $W(np)_2(O_2CMe)_2(S_2CNEt_2)_2$ Molecule

A	B	distance
W(1)	W(2)	2.2909 (16)
W(1)	S(3)	2.517 (3)
W(1)	S(5)	2.538 (3)
W(1)	O(29)	2.165 (6)
W(1)	O(33)	2.144 (6)
W(1)	C(19)	2.189 (9)
W(2)	S(11)	2.5252 (28)
W(2)	S(13)	2.517 (3)
W(2)	O(31)	2.150 (6)
W(2)	O(35)	2.149 (6)
W(2)	C(24)	2.198 (9)
S(3)	C(4)	1.695 (10)
S(5)	C(4)	1.733 (9)
S(11)	C(12)	1.705 (10)
S(13)	C(12)	1.716 (10)
O(29)	C(30)	1.283 (11)
O(31)	C(30)	1.263 (11)
O(33)	C(34)	1.275 (11)
O(35)	C(34)	1.248 (11)
N(6)	C(4)	1.327 (12)
N(6)	C(7)	1.476 (13)
N(6)	C(9)	1.484 (13)
N(14)	C(12)	1.328 (12)
N(14)	C(15)	1.472 (13)
N(14)	C(17)	1.476 (13)

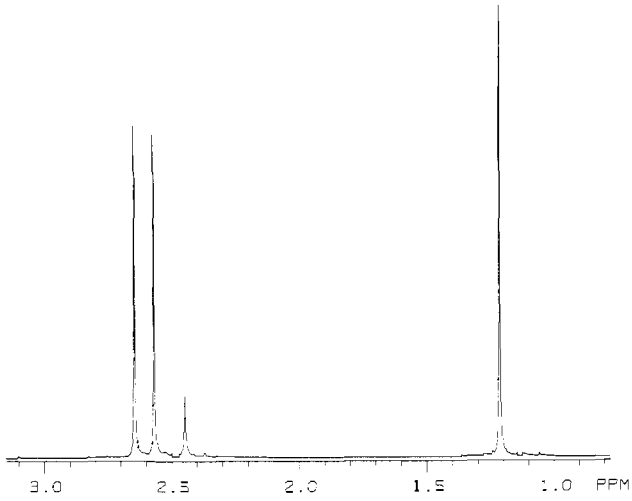

Figure 3. ^1H NMR spectrum of $W_2(np)_2(O_2CNMe_2)_4$ in benzene-d_6 recorded at 22 °C and 360 MHz.

signals in the ^1H NMR at 22 °C; see Figure 3. (Clearly mutually syn-neopentyl ligands are not disfavored on steric grounds.) When the sample was heated to 80 °C, the two carbamate signals coalesced, and at 100 °C a single resonance began to appear. This shows that $\Delta G^{\ddagger}$ for bridge–chelate exchange is ca. 17.9 ± 0.2 kcal/mol.

Synthesis of $W_2(np)_2(O_2CMe)_3(OSCMe)$. In an attempt to evaluate the role that sulfur has on the choice of structure, we began substituting carboxylate ligands with thioacetate ligands (CH_3COS^-). The initial product of these reactions provided a rather interesting molecule whose preparation is outlined in eq 2.

$$W_2(np)_2(O_2CMe)_4 + MeCOSH \xrightarrow[\text{toluene}]{25\ ^\circ C,\ 24\ h} W_2(np)_2(O_2CMe)_3(OSCMe) + MeCO_2H \quad (2)$$

The air-stable, crystalline, green solid can be prepared in near-quantitative yields based on eq 2.

Upon further reaction with excess thioacetic acid at elevated temperatures, a mixture of products and isomers was obtained. Even when all acetate ligands appear to have been replaced, isomers result from the various combinations of bridging thioacetate groups (i.e., the relative disposition of S and O at each W atom, $O_xS_{4-x}W{\equiv}WS_xO_{4-x}$, where x = 0–4), and each isomer appears to have axially coordinated alkyl ligands as judged by ^1H NMR studies which reveal ^{183}W coupling to the protons on the α carbons of the alkyl ligand. In molecules that adopt structure type II, ^{183}W coupling to the protons on the α carbons of the alkyl ligands is too small to be resolved, whereas molecules that adopt structure type I show coupling in the range 8–20 Hz.[1] We shall not discuss further these compounds in this paper, but will limit our discussion to the monosubstituted compound.

Proposed Molecular Structure of $W_2(np)_2(O_2CMe)_3(OSCMe)$. The proposed structure of $W_2(np)_2(O_2CMe)_3(OSCMe)$ is represented by III. In this molecule the asymmetry of the thioacetate ligand reduces the symmetry of the entire molecule to C_s.

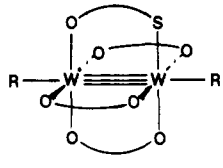

III

The ^1H NMR spectrum of $W_2(np)_2(O_2CMe)_3(OSCMe)$ is shown in Figure 4. There are two different neopentyl ligands as well as two different acetate signals in a 2:1 ratio, which is consistent with III. The methylene protons of the neopentyl ligands show $^3J_{WH}$ = 8.5 and 10.0 Hz. The methyl resonance of the thioacetate ligand occurs downfield of the acetate resonances at 3.26 ppm.[10]

Table III. Selected Bond Angles (Deg) for the $W_2(np)_2(O_2CMe)_2(S_2CNEt_2)_2$ Molecule

A	B	C	angle
W(2)	W(1)	S(3)	104.58 (6)
W(2)	W(1)	S(5)	109.96 (7)
W(2)	W(1)	O(29)	88.33 (18)
W(2)	W(1)	O(33)	88.73 (17)
W(2)	W(1)	C(19)	106.51 (21)
S(3)	W(1)	S(5)	68.33 (8)
S(3)	W(1)	O(29)	138.27 (18)
S(3)	W(1)	O(33)	70.50 (17)
S(3)	W(1)	C(19)	133.34 (26)
S(5)	W(1)	O(29)	69.96 (18)
S(5)	W(1)	O(33)	137.83 (17)
S(5)	W(1)	C(19)	128.78 (25)
O(29)	W(1)	O(33)	150.58 (23)
O(29)	W(1)	C(19)	76.5 (3)
O(33)	W(1)	C(19)	76.3 (3)
W(1)	W(2)	S(11)	102.38 (7)
W(1)	W(2)	S(13)	106.72 (6)
W(1)	W(2)	O(31)	89.95 (18)
W(1)	W(2)	O(35)	89.04 (17)
W(1)	W(2)	C(24)	104.57 (24)
S(11)	W(2)	S(13)	68.55 (9)
W(11)	W(2)	O(31)	70.47 (18)
S(11)	W(2)	O(35)	137.38 (18)
S(11)	W(2)	C(24)	136.60 (26)
S(13)	W(2)	O(31)	138.13 (17)
S(13)	W(2)	O(35)	68.84 (18)
S(13)	W(2)	C(24)	132.14 (25)
O(31)	W(2)	O(35)	151.44 (23)
O(31)	W(2)	C(24)	76.2 (3)
O(35)	W(2)	C(24)	76.5 (3)
W(1)	S(3)	C(4)	90.5 (3)
W(1)	S(5)	C(4)	88.9 (3)
W(2)	S(11)	C(12)	89.3 (3)
W(2)	S(13)	C(12)	89.4 (3)
W(1)	O(29)	C(30)	119.0 (6)
W(2)	O(31)	C(30)	118.7 (6)
W(1)	O(33)	C(34)	119.2 (6)
W(2)	O(35)	C(34)	118.9 (6)
C(4)	N(6)	C(7)	123.8 (8)
C(4)	N(6)	C(9)	118.7 (8)
C(7)	N(6)	C(9)	117.0 (8)
C(12)	N(14)	C(15)	120.5 (8)
C(12)	N(14)	C(17)	120.4 (8)
C(15)	N(14)	C(17)	118.7 (8)
S(3)	C(4)	S(5)	111.8 (5)
S(3)	C(4)	N(6)	125.1 (7)
S(5)	C(4)	N(6)	123.1 (7)
S(11)	C(12)	S(13)	112.2 (5)
S(11)	C(12)	N(14)	124.2 (8)
S(13)	C(12)	N(14)	123.5 (8)
W(1)	C(19)	C(20)	116.1 (6)
W(2)	C(24)	C(25)	115.9 (6)
O(29)	C(30)	O(31)	123.2 (8)
O(29)	C(30)	C(32)	116.9 (8)
O(31)	C(30)	C(32)	119.8 (8)
O(33)	C(34)	O(35)	123.1 (9)
O(33)	C(34)	C(36)	117.9 (9)
O(35)	C(34)	C(36)	119.0 (9)

Electronic Absorption Spectra. The electronic absorption spectrum of $W_2(np)_2(O_2CMe)_3(OSCMe)$ is also consistent with III since it reflects the valence $\pi^4\delta^2$ electronic configuration. (In the previous paper we gave a detailed analysis of the electronic absorption spectra of the $\pi^4\delta^2$ triple bonds in type I compounds.[1]) The most distinguishing characteristics of the absorption spectrum are the appearance of the triplet $\delta \rightarrow \delta^*$ transition at 16 500 cm^{-1} ($\epsilon = 3.1 \times 10^1$ M^{-1} cm^{-1}), the $\sigma_{wc} \rightarrow \sigma_{wc}^*$ transition at 32 700

(10) The chemical shift of the methyl resonance of CH_3COSH occurs at 2.41 ppm whereas in CH_3CO_2H it occurs at 2.11 ppm. Pouchert, C. J. *The Aldrich Library of NMR Spectra*, 2nd ed.; Aldrich Chemical Co.: Milwaukee, WI, 1983; Vol. 1.

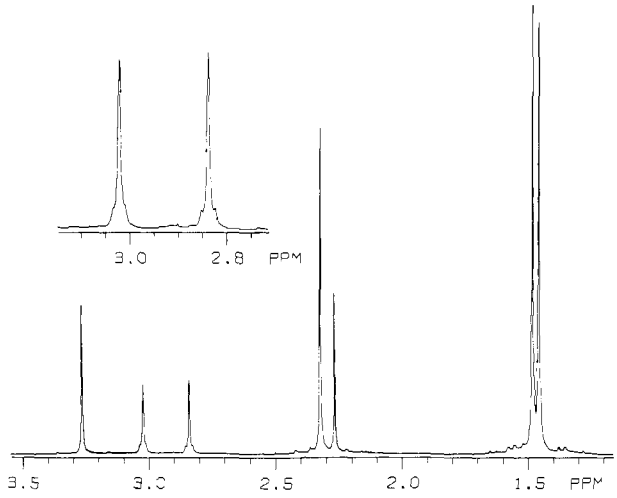

Figure 4. ^1H NMR spectrum of $W_2(np)_2(O_2CMe)_3(OSCMe)$ in benzene-d_6 at 22 °C and 360 MHz. The inset shows the methylene resonances of the neopentyl ligands, emphasizing the coupling to ^{183}W, $I = {}^1/_2$, 14.5% natural abundance with $^2J_{WH}$ = 8.5 and 10.0 Hz, respectively.

cm^{-1} ($\epsilon = 3.9 \times 10^4$ M^{-1} cm^{-1}), and the $\pi \rightarrow \pi^*$ transition at 40 300 cm^{-1} ($\epsilon = 1.0 \times 10^4$ M^{-1} cm^{-1}). These transitions are at similar energies and intensities to those observed in type I complexes of formula $W_2R_2(O_2CR')_4$. The singlet $\delta \rightarrow \delta^*$ transition is not observed in this compound but is obscured by a new transition, presumably the $\delta \rightarrow \pi^*_{sco}$ MLCT transition, at 28 300 cm^{-1} ($\epsilon = 6.4 \times 10^3$ M^{-1} cm^{-1}).

The electronic absorption spectra of both $W_2(np)_2(O_2CMe)_2(S_2CNEt_2)_2$ and $W_2(np)_2(O_2CNMe_2)_4$ recorded in CH_2Cl_2 solution at room temperature are consistent with these compounds containing valence $\sigma^2\pi^4$ electronic configurations. Most notable is the absence of any transition assignable to the $\delta \rightarrow \delta^*$ transition. For $W_2(np)_2(O_2CNMe_2)_4$ the first absorption maxima occur at 24 400 cm^{-1} (ϵ = 500 M^{-1} cm^{-1}) and 32 300 cm^{-1} (ϵ = 1000 M^{-1} cm^{-1}). In fact, this spectrum shows a striking similarity to spectra of other d^3–d^3 dimers of $\sigma^2\pi^4$ valence MO configuration such as $W_2(O\text{-}t\text{-}Bu)_6$, which shows absorption maxima at 21 000 cm^{-1} (ϵ = 800 M^{-1} cm^{-1}) and 27 000 cm^{-1} (ϵ = 2000 M^{-1} cm^{-1}). For $W_2(np)_2(O_2CMe)_2(S_2CNEt_2)_2$ absorption maxima occur at 27 200 cm^{-1} (ϵ = 3000 M^{-1} cm^{-1}) and 33 800 cm^{-1} (ϵ = 8000 M^{-1} cm^{-1}). In addition, two intense bands occur at 37 300 cm^{-1} (ϵ = 25 000 M^{-1} cm^{-1}) and 39 700 (ϵ = 29 000 M^{-1} cm^{-1}). Since these transitions are not present in the spectrum of $W_2(np)_2(O_2CNMe_2)_4$, we tentatively assign these to S-based charge-transfer transitions, which could be either MLCT (as seen for the carboxylates) or LMCT.

Bonding Considerations. The bonding in the new compound $W_2(np)_2(O_2CMe)_2(S_2CNEt_2)_2$ must parallel that described previously for $W_2Me_2(O_2CNEt_2)_4$,[7] in which five tungsten orbitals, s, p_x, p_y, $d_{x^2-y^2}$, and d_{xy}, are involved in forming metal–ligand σ bonds and metal d_{z^2}, d_{xz}, and d_{yz} form the M–M triple bond, $\sigma^2\pi^4$. There is, of course, the possibility for a mixing of s, d_{z^2}, and p_z atomic orbitals in the M–M σ bond, and the d_{z^2} doughnut can also be used in M–L σ bonding. Despite this "σ problem" it is clear that the M–M triple bonds in $W_2R_2(O_2CNR'_2)_4$ (R = Me, Bz, np; R′ = Me, Et) and $W_2(np)_2(O_2CMe)_2(S_2CNEt_2)_2$ are similar in nature to the M–M triple bonds in W_2^{6+}-containing compounds where the W atoms are three- or four-coordinate, e.g., $W_2(NMe_2)_6$,[11] $W_2(O\text{-}t\text{-}Bu)_6$,[12] W_2(pinacolate)$_3$,[13] $W_2(O\text{-}i\text{-}Pr)_6(py)_2$,[12] or $W_2(NMe_2)_4(ArN_3Ar)_2$.[14] All these compounds have W–W distances of ca. 2.30 Å, which are longer by ca. 0.1 Å than those in $W_2R_2(O_2CR')_4$ compounds of structure type I. See Table IV. We believe, therefore, that we must look for an electronic origin influencing the preference of structures II relative to I.

Table IV. Comparison of W–W Triple-Bond Distances (Å) in Compounds Having Valence MO Descriptions $\sigma^2\pi^4$ and $\pi^4\delta^2$

compd	W–W distance	MO config	ref
$W_2(np)_2(O_2CEt)_4$	2.1911 (7)	$\pi^4\delta^2$	*a*
$W_2(Bz)_2(O_2CEt)_4$	2.1859 (12)	$\pi^4\delta^2$	*a*
$W_2(np)_2(O_2CMe)_2(S_2CNEt_2)_2$	2.2909 (16)	$\sigma^2\pi^4$	*b*
$W_2Me_4(O_2CNEt_2)_4$	2.272 (1)	$\sigma^2\pi^4$	*c*
$W_2(OCMe_2CMe_2O)_3$	2.2738 (8)	$\sigma^2\pi^4$	*d*
$W_2(O\text{-}i\text{-}Pr)_6(py)_2$	2.334 (1)	$\sigma^2\pi^4$	*e*
$W_2(O_2C\text{-}t\text{-}Bu)_6$	2.2922 (8)	$\sigma^2\pi^4$	*f*
$W_2(NMe_2)_6$	2.294 (1)	$\sigma^2\pi^4$	*g*
$W_2(O_2CNMe_2)_6$	2.279 (1)	$\sigma^2\pi^4$	*c*
$W_2(CH_2SiMe_3)_6$	2.255 (2)	$\sigma^2\pi^4$	*h*

[a] Reference 1. [b] This work. [c] Reference 7. [d] Reference 13. [e] Akiyama, M.; Chisholm, M. H.; Cotton, F. A.; Extine, M. W.; Haitko, D. A.; Little, D.; Fanwick, P. E. *Inorg. Chem.* **1979**, *18*, 2266. [f] Chisholm, M. H.; Heppert, J. A.; Hoffman, D. M.; Huffman, J. C. *Inorg. Chem.* **1985**, *24*, 3214. [g] Reference 11. [h] Chisholm, M. H.; Cotton, F. A.; Extine, M. W.; Stults, B. R. *Inorg. Chem.* **1979**, *98*, 6046.

Scheme I

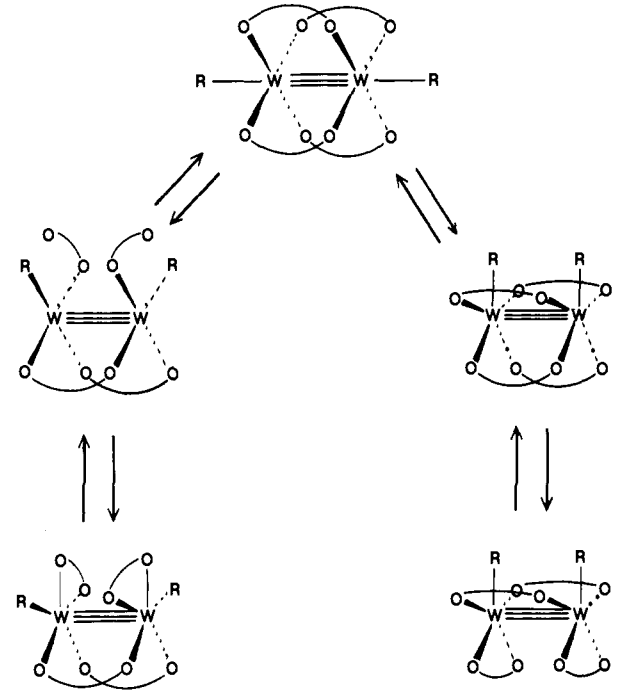

^1H NMR studies on compounds of formula $W_2(CH_2R)_2(O_2CR')_4$ (R = Ph; R′ = H, Me, Et) indicate an equilibrium mixture of I and II exists in solution.[1] The isomers I and II must be very close in energy for R and R′ = alkyl or aryl. For the carbamates, $W_2R_2(O_2CNR'_2)_4$, and the dithiocarbamate molecule reported here, the energy minimum clearly lies in the favor of II, with the M–M configuration $\sigma^2\pi^4$ being favored relative to I with $\pi^4\delta^2$.

Two questions are raised by these observations. (1) For the $W_2R_2(O_2CR')_4$ compounds that exist in equilibrium, I $\rightleftharpoons$ II, what reaction coordinate allows for this interconversion? (2) For $W_2R_2(O_2CNR'_2)_4$ compounds, what is the influence of replacing an amido group for an alkyl or aryl group? Let us now address these questions in the above order.

Interconverting Isomers I and II. It is possible that a carboxylate ligand "arm-off" reaction creates a vacant coordination site in an equatorial position which provides an opportunity for W–R bond migration, axial → equatorial. However, this arm-off process would have to be repeated and reversed several times to allow for

(11) Chisholm, M. H.; Cotton, F. A.; Extine, M. W.; Stults, B. R. *J. Am. Chem. Soc.* **1976**, *98*, 4477.
(12) Akiyama, M.; Chisholm, M. H.; Cotton, F. A.; Extine, M. W.; Haitko, D. A.; Little, D.; Fanwick, P. E. *Inorg. Chem.* **1979**, *18*, 2266.
(13) (a) Chisholm, M. H.; Folting, K.; Hampden-Smith, M.; Smith, C. A. *Polyhedron* **1987**, *6*, 1747. (b) Smith, C. A. Ph.D. Thesis, Indiana University, 1985.
(14) Chisholm, M. H.; Folting, K.; Haitko, D. A.; Huffman, J. C. *Inorg. Chem.* **1981**, *20*, 171.

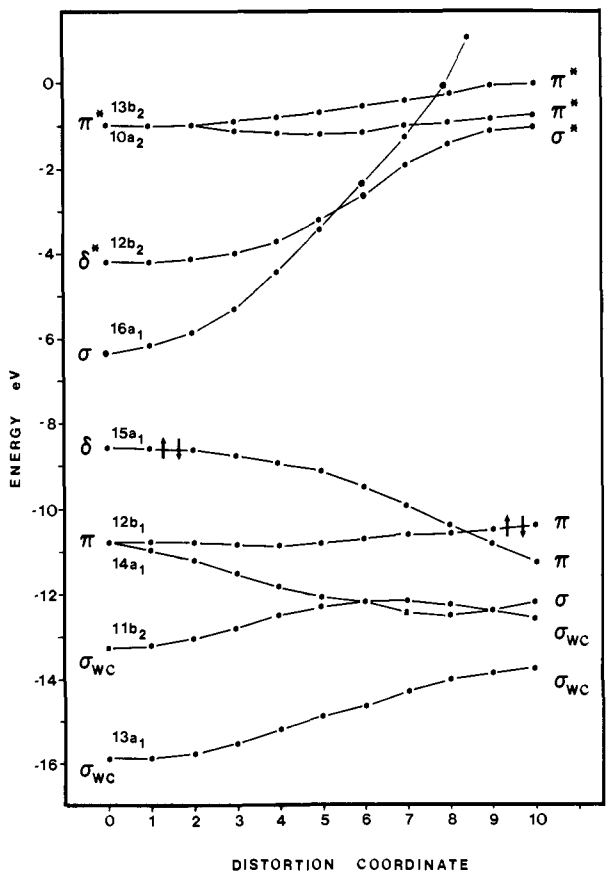

Figure 5. Walsh diagram for the concerted distortion between axial (left) to equatorial (right) isomers of $W_2(CH_3)_2(O_2CH)_4$ while preserving C_{2v} symmetry. The HOMOs are denoted by arrows. The labels σ, π, and δ refer to the character of predominantly metal-based orbitals. The label σ_{wc} refers to the W–C σ-bonding orbitals.

the conversion of I to II since the alkyl ligands in II are mutually syn. It is therefore attractive to consider an alternate mechanism in which bonds are not necessarily broken. Specifically, is a concerted reaction pathway possible in which C_{2v} symmetry is maintained? These two types of reaction pathways are qualitatively depicted in Scheme I. On the left-hand side the "arm-off" carboxylate ligand reaction profile shows how other isomers (i.e., those in which the W–R bonds are not mutually syn) can easily arise. On the right-hand side the initial concerted reaction interconverts the axial and syn W–R groups followed by a bridge–bidentate carboxylate group site exchange. For $W_2R_2(O_2CNMe_2)_4$ compounds such exchange of O_2CNMe_2 ligands occurs on the NMR time scale. The detailed mechanism for the latter is not known and could occur by either carboxylate "arm-off" or W–O bridge formation. We have not found any solvent dependence on the rate of this fluxional process, which causes us to consider the possibility of the concerted reaction pathway as a viable process.

We have chosen to investigate the possibility of such a concerted distortion by performing Fenske–Hall calculations on the model system $W_2(CH_3)_2(O_2CH)_4$ with the restriction of preserving C_{2v} symmetry. The distortion coordinate consists of 11 synchronous regular variations of bond angles and dihedral angles while maintaining C_{2v} symmetry. One last calculation was performed on a "relaxed" molecule in which the W–W distance was lengthened by ca. 0.1 Å and with both chelating and bridging carboxylate ligands. This revealed that the essential bonding picture is relatively unaffected by the W–W "relaxation" and presence of chelating ligands.

Tracing the Basic Distortion. A Walsh diagram for the concerted C_{2v} distortion is displayed in Figure 5. On the left side of the Walsh diagram in Figure 5 are the important MOs of "axial" geometry (type I) and on the right are those of "equatorial"

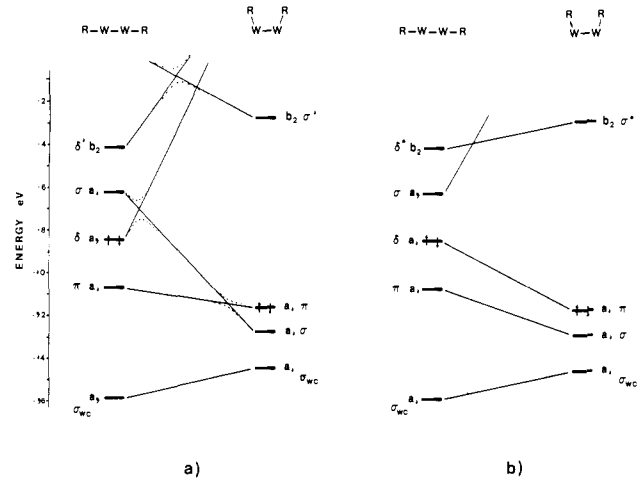

Figure 6. Correlation of molecular orbitals of axial and equatorial isomers of C_{2v}-$W_2(CH_3)_2(O_2CH)_4$ showing only the important a_1 and b_2 orbitals: (a) before and (b) after, taking avoided crossings into account. For each of (a) and (b) the orbitals on the left are for $\pi^4\delta^2$ configurations and the orbitals on the right are for $\sigma^2\pi^4$ configurations.

geometry (type II) for the model compound $W_2(CH_3)_2(O_2CH)_4$ under C_{2v} symmetry. The HOMO of each geometry is denoted by arrows. The "axial" type I geometry (left) gives rise to an approximate valence MO description of $\pi^4\delta^2$, whereas the "equatorial" type II geometry (right) yields the expected $\sigma^2\pi^4$ configuration.[15] We see that the distortion dramatically increases the magnitude of the HOMO–LUMO gap, and most important is that the Walsh diagram reveals that there is essentially no electronic energy barrier for the interconversion of $\pi^4\delta^2$ and $\sigma^2\pi^4$ valence M–M MO configurations.

Let us now take a more detailed look at the actual transformation of I to II. A simplified orbital correspondence between I and II based on orbital composition, without taking into account the avoided crossings, is given for the predominantly metal-based a_1 and b_2 orbitals in Figure 6a. In the course of the distortion, the a_1 W–W π-bonding and W–C σ-bonding orbitals maintain their composition, and their orbital energies are relatively unperturbed between the I (left) and II (right) geometries. In contrast, the occupied a_1 W–W δ-bonding orbital of I (left) corresponds with the unoccupied δ orbital in II (right). In a similar fashion, the unoccupied a_1 W–W σ-bonding orbital of I (left) corresponds to the occupied W–W σ-bonding orbital of isomer II (right). Since a ground reactant state correlates with a doubly excited product state, the interconversion of $\pi^4\delta^2$ and $\sigma^2\pi^4$ configuration is formally forbidden in a Woodward–Hoffmann sense.[16] However, under C_{2v} symmetry both σ and δ MOs have the same symmetry and their crossing is avoided. Taking into account the necessary avoidance of orbitals of the same symmetry, we arrive at the approximate correlations of Figure 6b. The occupied a_1 π of I correlates with a_1 σ or II, and the unoccupied b_2 δ^* of I correlates with the unoccupied b_2 σ^* orbital in II. In reality, other avoided crossings occur (between both metal- and ligand-based orbitals) because there are other orbitals of the same symmetry, but the essence of the distortion is depicted here in simplified form.

(15) It is interesting to compare the results of extended-Hückel, Fenske–Hall, and relativistic Xα–SW calculations on the model compound $W_2(CH_3)_2(O_2CH)_4$ in an "axial" type I geometry. The extended-Hückel results[17] give essentially the same result presented here for the Fenske–Hall calculations in that the unoccupied M–M σ orbital is calculated to be the LUMO with the unoccupied δ^* orbital higher in energy. The Xα–SW results reverse this ordering and predict the δ^* orbital to be the LUMO with the unoccupied σ orbital higher in energy. The Xα results were shown[1] to be in better agreement with the spectroscopic data; however, the actual energetic placement of the unoccupied M–M σ orbital has no bearing on the "allowedness" of the interconversion between $\pi^4\delta^2$ and $\sigma^2\pi^4$ configurations. See Braydich et al. for Xα results (Braydich, M. D.; Bursten, B. E.; Chisholm, M. H.; Clark, D. L. *J. Am. Chem. Soc.* **1985**, *107*, 4459).

(16) Woodward, R. B.; Hoffmann, R. *The Conservation of Orbital Symmetry*; Academic: New York, 1970; *Angew. Chem., Int. Ed. Engl.* **1969**, *8*, 781.

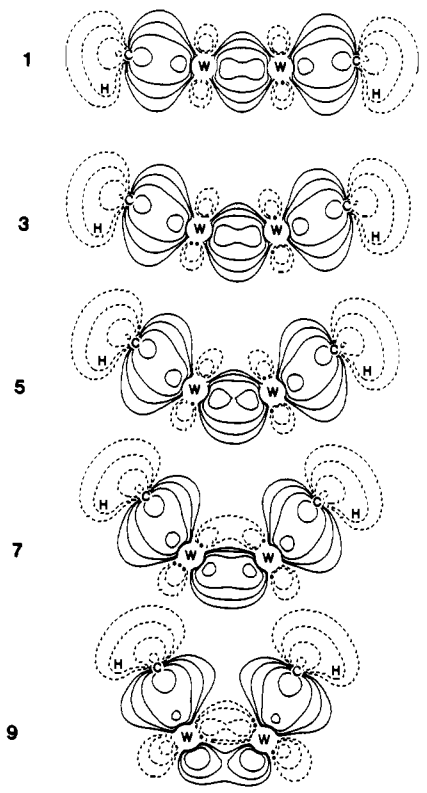

Figure 7. Contour plots tracing the rehybridization of the a_1 W–C σ-bonding orbital along the distortion coordinate. Numbers on the left refer to the actual points along the distortion coordinate from type I (top) to type II (bottom). These and all subsequent plots are in the horizontal mirror plane containing the W atoms, the axial C atoms, and two of the C–H bonds. Contour values for this and all subsequent plots are ±0.02, ±0.04, ±0.08, and ±0.16 e/Å^3. Dashed lines represent negative density contours and solid lines represent positive density contours.

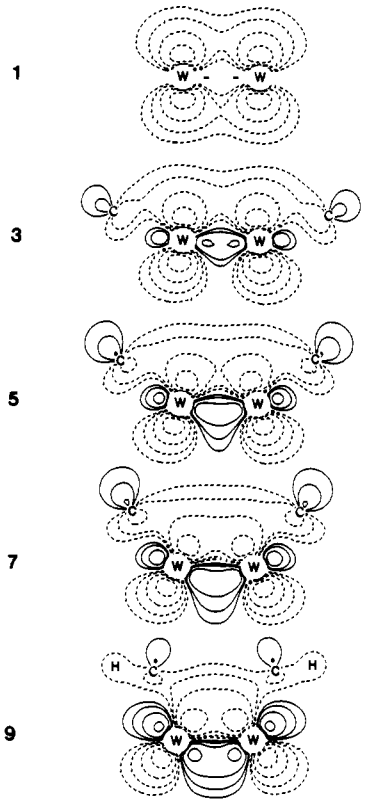

Figure 8. Contour plots tracing the rehybridization of predominantly W–W δ to W–W π along the distortion coordinate.

For the interconversion of $\pi^4\delta^2$ and $\sigma^2\pi^4$ triple bonds, the occupied δ and unoccupied σ orbitals lie close in energy and the avoided crossing occurs so early along the distortion coordinate that the one-electron barrier is very small as seen in the Walsh diagram of Figure 5. For many organic systems, the remnants of such intended but avoided crossings appear as large energy barriers that reflect the inherent forbiddenness of the reaction. Two-electron effects introduced by configuration interaction (to give proper states) could wipe out the barrier completely.[17] For the interconversion of I $\rightleftharpoons$ II, the lowest state configuration of the transition-state complex ($\pi^4\delta^2$) and the doubly excited configuration of the transition-state complex ($\pi^4\sigma^2$) both have $^1A_1$ symmetry, should be similar in energy, and are expected to mix appreciably. In contrast to many organic systems,[17] this should only involve a small energy expenditure. In other words, configuration interaction can effectively remove the forbiddenness of the distortion, and the interconversion of $\pi^4\delta^2$ to $\sigma^2\pi^4$ W≡W bonds is perhaps more appropriately described as "state allowed".

The avoidance of orbitals of the same symmetry along the distortion coordinate manifests itself as a rehybridization of metal-based orbitals as shown in the Walsh diagram of Figure 5 and the simplified correlation diagrams in Figure 6. One may ask how a M–M δ orbital can rehybridize into a M–M π and how a M–M π orbital can rehybridize into a M–M σ. Under C_{2v} symmetry the M–M σ, δ, and one of the M–M π orbitals all have a_1 symmetry and will thus be able to mix together upon distortion. From perturbation theory these levels will "repel" each other and the wave functions describing each of the new orbitals along the distortion coordinate will be a mixture of the old. As an illustrative example let us consider the rehybridization of the a_1 W–C σ-bonding orbital. In the "axial" type I geometry this orbital may be envisioned to arise from interaction between the M–M σ bond and the in-phase combination of R_2 orbitals as shown in **1**. In

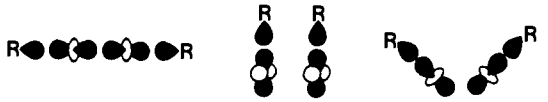

1 **2** **3**

contrast, the a_1 W–C σ-bonding orbital in type II complexes can be envisioned to arise from interaction of M–M δ with the in-phase combination of R_2 orbitals as shown in **2**. Now, at some point midway along the distortion coordinate the a_1 W–C σ-bonding orbital will be an admixture of the two extremes as depicted in **3**. We can reinforce this qualitative picture with the aid of contour plots of the a_1 W–C σ-bonding orbital taken as a slice through a plane containing the W_2R_2 moiety. Figure 7 illustrates this rehybridization of the a_1 W–C σ-bonding orbital with the use of contour plots taken at five points along the distortion coordinate. Thus the plots taken at points 1, 5, and 9 (Figure 7) correspond to our qualitative drawings shown above in **1**, **3**, and **2**, respectively. With the aid of contour plots, we also illustrate the rehybridization of M–M δ to M–M π in Figure 8 and M–M π to M–M σ in Figure 9.

Factors Influencing the Relative Stabilities of Isomers I and II. As noted earlier I and II may exist in equilibrium for certain $W_2R_2(O_2CR')_4$ compounds, indicating that the isomers are close to isoenergetic. Bulky combinations of R and R′ favor I while for R = R′ = Me, II is favored. For R = Bz and R′ = Et, the equilibrium position can be tipped by the choice of solvent. However, as we found before for $W_2Me_2(O_2CNEt_2)_4$ and show here for $W_2(np)_2(O_2CNMe_2)_4$ and $W_2Bz_2(O_2CNMe_2)_4$, the isomeric form II is favored exclusively. Subtle electronic factors are obviously capable of displacing the equilibrium toward II even when steric factors are operating in the reverse direction. This has prompted us to examine the influence of nitrogen lone-pair conjugation with the CO_2 moiety and the metal-based orbitals.

Effect of Conjugation on the $\pi^4\delta^2$ Manifold. In the preceding paper we showed that arene rings in $W_2R_2(O_2CAr)_4$ and W_2-

(17) For an excellent discussion, see: Salem, L. *Electrons in Chemical Reactions: First Principles*; Wiley: New York, 1981; Chapter 5 and references therein. We are grateful to a reviewer for bringing this to our attention.

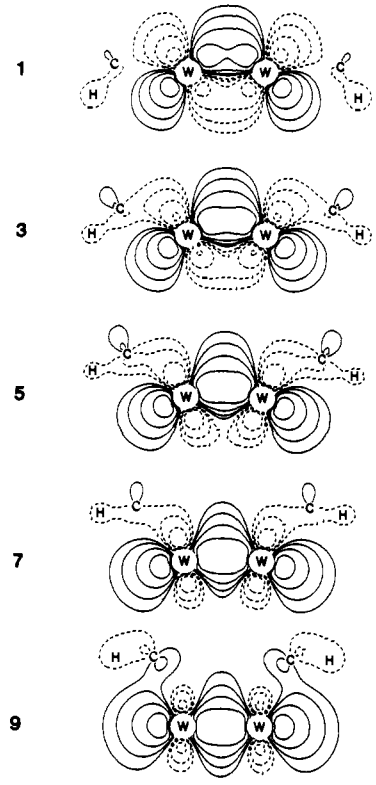

Figure 9. Contour plots tracing the rehybridization of predominantly W–W π to W–W σ along the distortion coordinate.

$(O_2CAr)_4$ compounds influence the carboxylate π system in $ArCO_2^-$ ligands and that this causes both a dramatic red shift and a splitting in the $\delta \rightarrow \pi^*_{oco}$ MLCT transition when compared to the alkyl carboxylates of type I.[1] Let us now consider the effect of substituting an NR_2 group to generate $R_2NCO_2^-$ ligands. In the ground-state structures there are planar C_2NCO_2 units, and ^1H NMR studies show restricted rotation about the central C–N bonds in solution for metal carbamate complexes.[18] These arguments can and will be extended to the $R_2NCS_2^-$ ligands.

To begin our discussion, let us turn to some simple group theoretical considerations. For quadruply bonded $W_2(O_2CX)_4$ compounds ($\sigma^2\pi^4\delta^2$), the set of four carboxylate π bonds of the individual carboxylate ligands form symmetry-adapted linear combinations of a_{2g}, b_{2g}, and e_u symmetry in the D_{4h} point group. Introduction of four NH_2 moieties coplanar with the carboxylate ligands introduces four N lone-pair orbitals also spanning a_{2g}, b_{2g}, and e_u representations, and these are expected to interact with the carboxylate π system. Now, if the NH_2 moieties are rotated by 90° such that the N lone-pair orbitals are perpendicular to the carboxylate π system, the N lone pairs span a_{2u}, b_{2u}, and e_g symmetry. In the latter situation, conjugation is rendered impossible by symmetry. The same arguments apply for $W_2R_2(O_2CX)_4$ species with the exception that we are now in the C_{2h} point group. When the carboxylate π and NH_2 lone-pair orbitals are coplanar, they span $2b_g$, a_u, and b_u representations. The M–M δ orbital has b_g symmetry and thus the b_g orbitals are expected to interact. When the NH_2 moieties are rotated by 90°, the N lone-pair combinations that were b_g are now b_u and thus can no longer interact by symmetry. Effectively these observations allow us to turn this conjugation either "on" or "off" and thereby examine its effects on the $\pi^4\delta^2$ manifold.

The results of Fenske–Hall calculations on the model compound $W_2(CH_3)_2(O_2CNH_2)_4$ of structural type I, shown in Figure 10, illustrate the effect of conjugation with the N lone-pair orbitals of b_g symmetry. Shown on the left of Figure 10 are the pertinent M–M bonding orbitals for the unconjugated form where the NH_2 units are perpendicular to the carboxylate units, and on the right

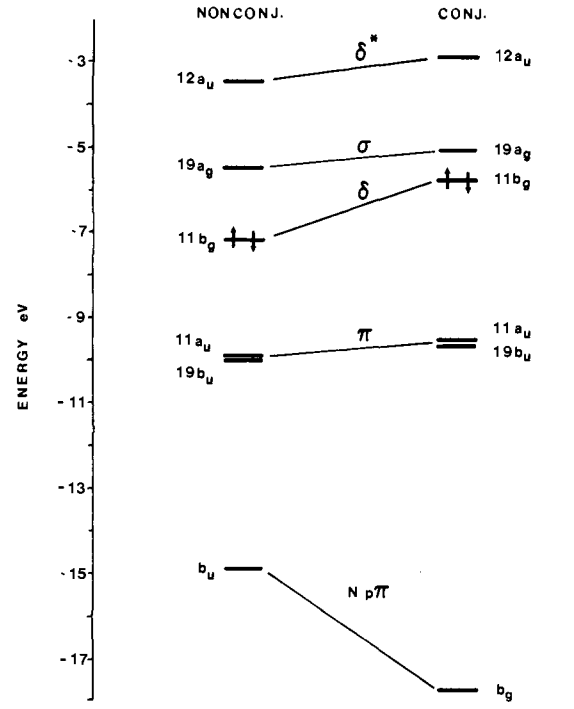

Figure 10. Correlation of molecular orbitals for $W_2(CH_3)_2(O_2CNH_2)_4$ of structural type I with the NH_2 moieties coplanar (right, conjugated) and perpendicular to (left, nonconjugated) the carboxylate π systems.

are the corresponding orbitals for the conjugated form where CO_2 and NH_2 units are coplanar. We obtain the expected approximate valence MO configuration of $\pi^4\delta^2$ for both conjugated and unconjugated forms of the molecule. Upon rotation of the NH_2 units from a perpendicular to a coplanar arrangement with respect to the carboxylate units, we observe a destabilization of the M–M δ-bonding b_g orbital and a concomitant stabilization of the b_g N lone-pair orbital as a result of conjugation. Clearly, introduction of carbamate ligands adds an additional electronic factor influencing the stability of structural type I compounds. Conjugation between the carboxylate π and N p π lone-pair orbitals has a destabilizing influence on the M–M δ-bonding orbital of type I compounds and decreases the magnitude of the HOMO–LUMO gap. Presumably this conjugation with N lone-pair orbitals raises the energy of the δ orbital enough to effectively tip the stability away from $\pi^4\delta^2$ and more toward $\sigma^2\pi^4$. Looking back to the Walsh diagram of Figure 5, we can imagine destabilizing δ by ca. 1.0 eV (as seen in Figure 10) to yield a much greater stabilization upon distortion to $\sigma^2\pi^4$. This same argument applies to the dithiocarbamate ligands of the compound $W_2(np)_2(O_2CMe)_2(S_2CNEt_2)_2$. The formation of $W_2(np)_2(OSCMe)_4$ complexes of $\pi^4\delta^2$ configuration indicates that S-based ligands have little effect on the $\pi^4\delta^2$ manifold. Thus we conclude that it is not the presence of S, but the presence of N lone-pairs in S_2CNR_2 ligands that prefers the $\sigma^2\pi^4$ configuration for the new compound $W_2(np)_2(O_2CMe)_2(S_2CNEt_2)_2$.

Concluding Remarks

The structural characterization of $W_2(np)_2(O_2CMe)_2(S_2CNEt_2)_2$ provides yet another example of a structural type II geometry where each tungsten atom forms five bonds in a pentagonal plane to five ligand atoms. The experimental data and the Fenske–Hall calculations are in agreement with a valence M–M MO configuration of $\sigma^2\pi^4$. The alternate structural type I has previously been shown to contain the valence M–M MO configuration of $\pi^4\delta^2$. We have shown that both steric and electronic factors appear to be important in influencing the choice of $\pi^4\delta^2$ or $\sigma^2\pi^4$ configurations for compounds of formula $W_2(R)_2(O_2CX)_4$. The importance of the steric bulk of supporting ligands appears to follow the order R > X. However, electronic factors can override steric factors as in the case where X = NR_2,

(18) Chisholm, M. H.; Extine, M. W. *J. Am. Chem. Soc.* **1977**, *99*, 782.

Table V

Structural Parameters for $W_2(CH_3)_2(O_2CH)_4$

types I, II		type I		type II	
atoms	length, Å	atoms	angle, deg	atoms	angle, deg
W–W	2.189	W–W–O	90.5	W–W–O[a]	89.8
W–C	2.190	W–O–C	118.6	W–W–O[b]	104.9
W–O	2.085	W–W–C	180.0	W–O–C[a]	118.6
O–C	1.270	W–C–H	113.2	W–O–C[b]	92.1
C–H	1.090	O–C–H	119.2	W–W–C	106.1
		H–C–H	109.0	W–C–H	113.2
				O–C–H[a]	118.25
				O–C–H[b]	122.0
				H–C–H	109.0

Structural Parameters for $W_2(CH_3)_2(O_2CNH_2)_4$

types I, II		type I		type II	
atoms	length, Å	atoms	angle, deg	atoms	angle, deg
W–W	2.189,[c] 2.272[d]	W–W–O	90.5	W–W–O[a]	89.8
W–C	2.190,[c] 2.201[d]	W–O–C	118.6	W–W–O[b]	104.9
W–O	2.085,[c] 2.075[d]	W–W–C	180.0	W–O–C[a]	118.6
O–C	1.270,[c] 1.285[d]	W–C–H	113.2	W–O–C[b]	92.1
C–H	1.090,[c] 1.090[d]	O–C–H	119.2	W–W–C	106.1
C–N	1.340,[c] 1.340[d]	H–C–H	109.0	W–C–H	113.2
N–H	1.010,[c] 1.010[d]	C–N–H	101.0	O–C–H[a]	118.25
				O–C–H[b]	122.0
				H–C–H	109.0
				C–N–H	101.0

[a] Bridging. [b] Chelating. [c] Type I. [d] Type II.

for which conjugation between carboxylate π, N lone-pair, and M–M δ orbitals results in a destabilization of the $\pi^4\delta^2$ configuration. Furthermore, we have shown that there is essentially no electronic energy barrier for interconversion between $\pi^4\delta^2$ and $\sigma^2\pi^4$ configurations of $W_2R_2(O_2CR')_4$ compounds, and the interconversion can be described as a "state-allowed" process. These observations have greatly renewed our interest in the fascinating coordination chemistry of $X_nM{\equiv}MX_n$-containing compounds where n = 5 or 6.[8]

Experimental and Computational Procedures

Computational Procedures. The coordinates for axial $W_2(CH_3)_2(O_2CH)_4$ were idealized to C_{2h} point symmetry, but otherwise bond lengths and angles were taken from the crystal structure of $W_2(CH_2Ph)_2(O_2CEt)_4$.[19] Identical coordinates were used for axial $W_2(CH_3)_2(O_2CNH_2)_4$ except that NH_2 units were introduced in place of H. Distances and angles of the bridging carbamate moiety were idealized from the bridging O_2CNEt_2 moiety in the crystal structure of $W_2(CH_3)_2(O_2CNEt_2)_4$.[7] Structural parameters for equatorial $W_2(CH_3)_2(O_2CX)_4$ (X = H, NH_2) were idealized to C_{2v} point symmetry but otherwise used bond lengths and angles from the crystal structure of $W_2(CH_3)_2(O_2CNEt_2)_4$.[7] A summary of the structural parameters employed in this study are given in Table V.

Approximate molecular orbital calculations were performed by using the Fenske–Hall method, which has been discussed in detail elsewhere.[20]

All atomic wave functions were generated by a best fit to Herman–Skillman atomic calculations by using the method of Bursten, Jensen, and Fenske.[21] Contracted double-ζ representations were used for W 5d AOs as well as for C, O, and N 2p AOs. Basis functions for the tungsten atom were derived for a +1 oxidation state with the valence 6s and 6p exponents fixed at 1.8. An exponent of 1.16 was used for the H 1s atomic orbital.[22]

All the calculations described in this paper were obtained at the Indiana University Computational Chemistry Center on a VAX 11/780 computer system, and contour plots were obtained on a Talaris 800 laser printer.

Physical Techniques. ^{1}H NMR spectra were recorded on a Nicolet NT-360 spectrometer at 360 MHz in dry and oxygen-free benzene-d_6. ^{1}H NMR chemical shifts are reported in ppm relative to the ^{1}H impurity in benzene-d_6 set at 7.15 ppm.

(19) Chisholm, M. H.; Hoffman, D. M.; Huffman, J. C.; Van Der Sluys, W. G.; Russo, S. *J. Am. Chem. Soc.* **1984**, *106*, 5386.
(20) Hall, M. B.; Fenske, R. F. *Inorg. Chem.* **1972**, *11*, 768.
(21) Bursten, B. E.; Jensen, J. R.; Fenske, R. F. *J. Chem. Phys.* **1978**, *68*, 3320.
(22) Hehre, W. J.; Stewart, R. F.; Pople, J. A. *J. Chem. Phys.* **1969**, *51*, 2657.

Table VI. Crystal Data for the $W_2(np)_2(O_2CMe)_2(S_2CNEt_2)_2$ Molecule

empirical formula	$W_2C_{22}H_{48}N_2O_4S_4$
color of crystal	orange
space group	$P2_1/a$
cell dimensions (at −160 °C; 30 reflections)	
a, Å	17.092 (12)
b, Å	11.023 (7)
c, Å	17.576 (12)
β, deg	98.19 (4)
Z (molecules/cell)	4
volume, Å^3	3277.59
calcd density, g/cm^3	1.825
wavelength, Å	0.71069
mol wt	900.57
linear absorption coeff, cm^{-1}	74.375
max abs	0.3710
min abs	0.6150
detector to sample dist, cm	22.5
sample to source dist, cm	23.5
takeoff angle, deg	2.0
average ω scan width at half-height, deg	0.25
scan speed, deg/min	4.0
scan width, deg	2.0 + dispersion
single background time at extremes, s	8
aperture size, mm	3.0 × 4.0
min 2θ, deg	6
max 2θ, deg	45
total no. of reflections	4562
no. of unique intensities	4562
no. with $F > 3.00\sigma(F)$	3626
$R(F)$	0.0341
$R_w(F)$	0.0360

Infrared spectra were recorded on a Perkin-Elmer 283 spectrometer as Nujol mulls between CsI salt plates and referenced to polystyrene at 1601 cm^{-1}.

Electronic absorption spectra were recorded on a Perkin-Elmer 330 spectrophotometer. Samples were run vs. a solvent blank using matched 1.00- or 0.10-cm quartz cells. Spectral grade solvents were used without further purification, except for degassing.

Elemental analyses were performed by Alfred Bernhardt Mikroanalytisches Laboratorium, Elbach, West Germany, and were handled under inert atmospheres.

Synthesis. All procedures were carried out under an atmosphere of dry and oxygen-free nitrogen using standard Schlenk and glovebox techniques. Starting materials were prepared according to the procedures given in the previous paper[1] or purchased from Aldrich.

$W_2(np)_2(O_2CMe)_2(S_2CNEt_2)_2$. In a Schlenk flask $W_2(np)_2(O_2CMe)_4$ (0.50 g, 0.67 mmol) was dissolved in toluene. To this was added slightly greater than 2 equiv of NaS_2CNEt_2 (0.24 g, 1.4 mmol) using a solids addition tube. At that point no reaction occurred until a small amount (ca. 10 μL) of dry glacial acetic acid was added. The reaction mixture began to turn orange within 1 min, and the solution was stirred for 24 h. The solvent was removed in vacuo and hexane was added. The crude product was filtered to remove NaO_2CMe. The solvent was then removed under reduced pressure to give an orange-yellow, microcrystalline solid (yield 0.51 g, 83%). Recrystallization from toluene produced large orange cubes. This compound is air stable for short periods of time in the solid state. Anal. Calcd for $W_2C_{24}H_{44}O_4S_4N_2$: C, 31.31; H, 4.83; N, 3.04. Found: C, 31.50; H, 5.00; N, 3.04.

^{1}H NMR (22 °C, benzene-d_6): δ 3.26 (q, $^3J_{HH}$ = 7.2 Hz, N(CH_2CH_3)$_2$), 2.68 (s, $^2J_{WH}$ < 4 Hz, CH_2CMe_3), 2.11 (s, O_2CMe), 1.33 (s, CH_2CMe_3), 0.81 (t, $^3J_{HH}$ = 7.2 Hz, N(CH_2CH_3)$_2$).

IR: 565 (vw), 580 (vw), 600 (w), 679 (s), 720 (mw), 732 (mw), 775 (mw), 851 (m), 917 (m), 1000 (mw), 1010 (m), 1062 (w), 1071 (mw), 1087 (m), 1150 (ms), 1211 (s), 1226 (m), 1275 (s), 1282 (s), 1301 (m), 1345 (w), 1358 (s), 1450 (vs), 1503 (vs), 1510 (vs), 1548 (s), 1560 (mw) cm^{-1}. Fluorolube: 1345 (w), 1355 (m), 1377 (w), 1390 (w), 1434 (s), 1450 (s), 1460 (ms), 1502 (s), 1509 (s), 1547 (ms) cm^{-1}.

$W_2(np)_2(O_2CMe)_3(OSCMe)$. In a Schlenk flask $W_2(np)_2(O_2CMe)_4$ (0.50 g, 0.67 mmol) was dissolved in toluene. To this was added a large excess (>4 equiv) of thioacetic *O*-acid. The solution was stirred for 24 h, during which time it became dark green-orange. The solvent was removed under reduced pressure to produce a dark green solid (0.47 g, 92%). Recrystallization from toluene produced large crystals. This compound is air stable both as a solid and in solution. Anal. Calcd for $W_2C_{18}H_{30}O_7S$: C, 28.52; H, 4.00; N, 0.00. Found: C, 28.52; H, 4.28; N, <0.02.

^{1}H NMR (22 °C, benzene-d_6): δ 3.26 (s, OSC*Me*), 3.03 (s, $^2J_{WH}$ = 8.54 Hz, C*H*$_2$CMe$_3$ next to S), 2.85 (s, $^2J_{WH}$ = 9.98 Hz, C*H*$_2$CMe$_3$ next to O), 2.32 (s, O$_2$C*Me*), 2.26 (s, O$_2$C*Me* trans to OSCMe) 1.49, 1.46 (s, CH$_2$C*Me*$_3$).

IR: 324 (m), 333 (m), 375 (w), 450 (w), 620 (w), 627 (w), 668 (ms), 680 (m), 907 (mw), 932 (w), 1018 (w), 1040 (w), 1088 (vs), 1175 (ms), 1202 (mw), 1236 (ms), 1349 (m), 1361 (ms), 1374 (ms), 1438 (vs), 1460 (s), 1492 (m) cm^{-1}.

W$_2$(np)$_2$(O$_2$CNMe$_2$)$_4$. In a Schlenk flask W$_2$(np)$_2$(NMe$_2$)$_4$ (0.30 g, 0.44 mmol) was dissolved in CH$_2$Cl$_2$ and then frozen in liquid N$_2$. A large excess (>4 equiv) of CO$_2$ was condensed into the flask. The solution was then slowly warmed to room temperature while the flask was connected to a Hg bubbler. The solvent was removed in vacuo to yield a yellow powder (0.35 g, 92%).

^{1}H NMR (22 °C, benzene-d_6): δ 2.66 (s, bridge O$_2$CN*Me*$_2$), 2.59 (s, chelate O$_2$CN*Me*$_2$), 2.46 (s, C*H*$_2$CMe$_3$), 1.23 (s, CH$_2$C*Me*$_3$).

IR: 212 (mw), 256 (m), 421 (m), 455 (m), 600 (mw), 615 (m), 651 (s), 669 (m), 696 (vw), 730 (ms), 748 (m), 769 (ms), 773 (ms), 778 (ms), 845 (mw), 872 (m), 995 (w), 1042 (m), 1060 (mw), 1091 (w), 1108 (vw), 1150 (vw), 1227 (m), 1268 (s, br), 1359 (m), 1410 (vs), 1500 (vs), 1570 (vw), 1610 (vs) cm^{-1}.

W$_2$Bz$_2$(O$_2$CNMe$_2$)$_4$. In a similar procedure a large excess of CO$_2$ was reacted with W$_2$Bz$_2$(NMe$_2$)$_4$.

^{1}H NMR (22 °C, benzene-d_6): δ 3.79 (s, C*H*$_2$Ph), 2.67, 2.28 s, O$_2$CN*Me*$_2$).

Crystallographic Studies. General operating procedures and listings of programs have been previously published.[23] Crystal data for W$_2$(np)$_2$(O$_2$CMe)$_2$(S$_2$CNEt$_2$)$_2$ are given in Table VI. A suitable crystal was transferred to the goniostat by standard inert-atmosphere handling techniques employed by the IUMSC and cooled to −160 °C with a gas-flow cooling system.

A systematic search of a limited hemisphere of reciprocal space located a set of diffraction maxima with systematic absences corresponding to the unique monoclinic space group $P2_1/a$. Subsequent solution and refinement confirmed this choice.

The structure was solved by a combination of direct methods (MULTAN78) and Fourier techniques and refined by full-matrix least squares. Many of the hydrogen atom positions were visible in a difference Fourier phased on the non-hydrogen parameters. The positions of all hydrogens were calculated and placed in fixed idealized positions (d(C–H) = 0.95 Å) for the final cycles. The hydrogen atoms were assigned a thermal parameter of 1 + B_{iso} of the carbon atom to which they were bound. The data were corrected for absorption for the final cycles of the refinement.

A final difference Fourier was essentially featureless, with the largest peak being 0.50 e/Å^3.

Acknowledgment. We thank Dr. D. M. Hoffman of Harvard University for helpful discussions and the National Science Foundation and the Wrubel Computing Center for support. D.L.C. gratefully acknowledges the support of a General Electric Foundation fellowship for 1985–1986.

Registry No. W$_2$(np)$_2$(O$_2$CMe)$_4$, 108603-67-4; W$_2$(np)$_2$(O$_2$CMe)$_2$(S$_2$CNEt$_2$)$_2$, 110097-42-2; W$_2$(np)$_2$(O$_2$CMe)$_3$(OSCMe), 110116-42-2; W$_2$(np)$_2$(NMe$_2$)$_4$, 72286-69-2; W$_2$(np)$_2$(O$_2$CNMe$_2$)$_4$, 72286-53-4; W$_2$Bz$_2$(NMe$_2$)$_4$, 82555-52-0; W$_2$Bz$_2$(O$_2$CNMe$_2$)$_4$, 84913-56-4; W$_2$(CH$_3$)$_2$(O$_2$CH)$_4$, 91549-49-4; W$_2$(CH$_3$)$_2$(O$_2$CNH$_2$)$_4$, 110097-43-3; NaS$_2$CNEt$_2$, 148-18-5; thioacetic acid, 507-09-5.

Supplementary Material Available: Anisotropic thermal parameters and a complete listing of bond distances and bond angles for the W$_2$(np)$_2$(O$_2$CMe)$_2$(S$_2$CNEt$_2$)$_2$ molecule (4 pages); F_o and F_c values for the same compound (10 pages). Ordering information is given on any current masthead page.

(23) Chisholm, M. H.; Folting, K.; Huffman, J. C.; Kirkpatrick, C. C. *Inorg. Chem.* **1984**, *23*, 1021.

Structure–Reactivity Relations for Thiol–Disulfide Interchange[1]

Janette Houk and George M. Whitesides*

Contribution from the Departments of Chemistry, Harvard University, Cambridge, Massachusetts 02138, and Massachusetts Institute of Technology, Cambridge, Massachusetts 02139. *Received February 5, 1987*

Abstract: Equilibrium constants were determined for thiol–disulfide interchange between 36 di- and trithiols and the disulfides derived from either 2-mercaptoethanol or dithiothreitol. Reactions were conducted in methanol-d_4/aqueous buffer (pH 7) or methanol-d_4 at 25 °C, using NMR spectroscopy to follow the reactions. These data were used to rank the dithiols in terms of reduction potential and to infer the structure of the disulfides formed from them on oxidation. There is a general correlation between the reducing ability of the dithiol and the size of the disulfide-containing ring formed on oxidation: dithiols that form six-membered rings are most strongly reducing (K = 10^3–10^5 M with respect to oxidized 2-mercaptoethanol); five- and seven-membered rings are approximately 1 order of magnitude less reducing. Compounds resembling 1,2-ethanedithiol form cyclic bis(disulfide) dimers in relatively dilute solutions (~1 mM) but polymerize at higher concentrations. Other classes of dithiols form polymers on oxidation.

The importance of the thiol–disulfide interchange reaction to biochemistry[2–8] and the remarkable ability of this reaction to effect the reversible cleavage and formation of strong, covalent S–S bonds at room temperature in aqueous solution[2–9] have prompted many studies of the physical-organic chemistry of this reaction.[10–17] These studies have established the reaction to be mechanistically simple. Interchange involves three steps (eq 1a–c): initial ionization of the thiol to thiolate anion, nucleophilic attack of the thiolate anion on a sulfur atom of the disulfide moiety, and

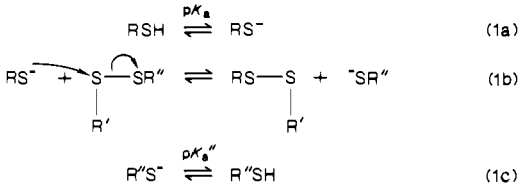

* To whom correspondence should be addressed at Harvard University.

(1) Supported by the National Institutes of Health, Grant GM 34411.
(2) Friedman, M. *The Chemistry and Biochemistry of the Sulfhydryl Group in Amino Acids, Peptides and Proteins*, 1st ed.; Pergamon: New York, 1973.
(3) Jocelyn, P. C. *Biochemistry of the SH Group*; Academic: New York, 1972.
(4) Torchinskii, Yu. M. *Sulfhydryl and Disulfide Groups of Proteins*; Plenum: New York, 1974.
(5) Fluharty, A. L. In *The Chemistry of the Thiol Group*; Patai, S., Ed.; Wiley: New York, 1974; p 589.
(6) Arias, I. M.; Jacoby, W. G. *Glutathione, Metabolism and Function*; Raven: New York, 1976.
(7) Kosower, N. S.; Kosower, E. M. In *Free Radicals in Biology*; Pryor, W. A., Ed.; Academic: New York, 1976; Vol. II, Chapter 2.
(8) Lin, T.-Y. In *The Proteins*, 3rd ed.; Neurath, H., Ed.; Academic: New York, 1977; Vol. III. Gilbert, H. F. *Methods Enzymol.* **1984**, *107*, 330.

0002-7863/87/1509-6825$01.50/0